JOURNAL OF CATALYSIS **167,** 172–179 (1997)
ARTICLE NO. CA971541

Vinylic Initiation of the Fischer–Tropsch Reaction over Ruthenium on Silica Catalysts

Helen C. Long, Michael L. Turner, Paolo Fornasiero,[1] Jan Kašpar,[1] Mauro Graziani,[1] and Peter M. Maitlis[2]

Department of Chemistry, The University of Sheffield, Sheffield, S3 7HF, United Kingdom

Received August 9, 1996; revised November 8, 1996; accepted November 11, 1996

Vinylic probes were added to a ruthenium-catalysed Fischer–Tropsch reaction in order to study the mechanism of hydrocarbon formation from CO/H_2. $^{13}C_2$ units derived from $^{13}CH_2{=}^{13}CHBr$ or $^{13}CH_2{=}^{13}CH_2$ are readily incorporated into the alkene and alkane products formed from ^{12}CO and H_2 over a Ru/SiO_2 catalyst (1 atm, 180°C). The levels of $^{13}C_2$ incorporation suggest that the probes are sources of $^{13}C_2$-labelled initiating units, proposed to be surface vinyls ($-CH{=}CH_2$). Further evidence for vinyl initiation is given by the increase in hydrocarbon formation rate during vinylic probe addition. This rate increase is not observed when ethyl bromide is added as a probe and shows the significance of the unsaturated initiating unit. $^{13}C_4$ incorporation in the C_4 hydrocarbon products (especially *cis*-2-butene) is attributed to a facile vinyl dimerisation reaction, as previously observed on rhodium catalysts and in discrete organometallic complexes. Hydrogenolysis of the $^{13}C_2$-probes was an appreciable side reaction over Ru/SiO_2 and resulted in some incorporation of $^{13}C_1$ units. © 1997 Academic Press

INTRODUCTION

The heterogeneously catalysed conversion of syn gas (CO and H_2) to hydrocarbons (the Fischer–Tropsch or FT reaction) is an industrially and academically interesting process. In a typical synthesis, syn gas is passed over a heated, supported metal catalyst at atmospheric pressure or above. The primary reaction products are 1-alkenes that undergo subsequent isomerisation and/or hydrogenation reactions to yield a complex mixture of hydrocarbons, predominantly linear alkenes and alkanes. Oxygen-containing products are also sometimes formed.

Analysis of the FT product distribution shows that Anderson–Schulz–Flory polymerisation kinetics are followed, in agreement with a reaction involving stepwise polymerisation of C_1 units. It is generally agreed today that the C_1 units are surface methylenes ($>CH_2$), formed by the hydrogenation of dissociated CO (1). The mechanism of the polymerisation has been the subject of considerable speculation. Fischer and Tropsch were the first to propose the involvement of surface methylene (2); this concept was developed by Pettit and Biloen and their collaborators who proposed an "alkyl mechanism" in which the chains grow by the insertion of a surface methylene into the M−C bond of a surface alkyl, and terminate by a β-hydride elimination from the surface alkyl to release the 1-alkene product (3–5). However, this theory has a number of shortcomings: it cannot easily account for the formation of small amounts of branched chain products or for the formation of anomalously low amounts of C_2 products. The β-hydride elimination step is also unexpected under such strongly hydrogenating conditions. We and others have felt that these are significant inadequacies that require a modification of the alkyl mechanism (6, 7).

Our early work on this topic involved the study of reactions of organometallic model complexes such as $[\{(Cp^*)Rh(CH_2)\}_2(Me)(L)]^+$ ($Cp^* = \eta^5\text{-}C_5Me_5$; $L =$ MeCN, etc.). This contains two bridging methylenes and one terminal methyl arranged about two rhodiums and was designed to resemble a portion of a rhodium catalyst during a FT synthesis (8). Decomposition of the complex gave propene by combination of the rhodium methyl and both methylene ligands; however, the study of ^{13}C- and D-labelled isotopomers showed that the propene was formed by a route in which a metal vinyl ($-CH{=}CH_2$), rather than a metal alkyl, was implicated as the key intermediate (9, 10). Oxidative decomposition of the complexes $[\{(Cp^*)Rh(\mu\text{-}CH_2)(CH{=}CHR)\}_2]$ ($Cp^* = \eta^5\text{-}C_5Me_5$; $R = H$, *cis*-Me) also led to facile coupling of an alkenyl group with a methylene (11, 12).

These data were reinforced by the work of others which showed that the coupling of sp^2 with sp^3 carbons in metal complexes was a lower energy process than a $Csp^3 + Csp^3$ coupling (13). In the context of the reactions of the dirhodium complexes, this suggested that an alkenyl + methylene (sp^2 with sp^3) coupling would be a lower energy process than an alkyl + methylene (sp^3 with sp^3) coupling. That prompted the question whether this could also hold true for reactions occurring over surfaces and hence

---

[1] Permanent address: Dipartimento di Scienze Chimiche, via L. Giorgieri 1, Universitá degli Studi di Trieste, 34100 Trieste, Italy.

[2] To whom correspondence should be addressed. Fax: +44-114-2738673. E-mail: P. Maitlis@Sheffield.ac.uk.

0021-9517/97 $25.00

whether surface alkenyls, rather than surface alkyls, were the chain carriers for CO hydrogenation over heterogeneous catalysts.

We investigated whether alkenyl or alkyl species participate in heterogeneous CO hydrogenation by adding sources of both vinyl and ethyl to a rhodium-catalysed FT reaction (14, 15). Rhodium was chosen as the catalyst since it matched the model systems; vinyl bromide, ethene, and ethyl bromide were used as probes since surface scientists had shown these molecules to be effective precursors of surface vinyl and ethyl, respectively, on clean metal surfaces (16–19). Addition of $^{13}C_2$-labelled probe molecules allowed the direct detection of probe incorporation into the hydrocarbon products by mass spectroscopic analysis, at levels of sensitivity that had not previously been obtained by other researchers. The doubly labelled probe also ensured that we could detect splitting of the probe molecules (and other probe reactions) and allowed us to define more clearly the roles of various species in the Fischer–Tropsch process.

We found that addition of vinylic probes to a rhodium-catalysed FT synthesis increased the formation rate of the $C_{\geq 2}$ (C_2 and higher) hydrocarbons; by contrast, addition of the ethyl probe increased only the C_2 formation rate. Addition of $^{13}CH_2{=}^{13}CHBr$ or of $^{13}CH_2{=}^{13}CH_2$ resulted in significant $^{13}C_2$ incorporation into the hydrocarbon products, at levels which compared favourably with those predicted by a mathematical model of C_2 initiation. $^{13}C_1$ and $^{13}C_3$ incorporation remained at natural abundance levels, showing that the probes were not cleaved under the catalytic conditions. In addition, we observed significant $^{13}C_4$ incorporation in the C_4 products, which was attributed to a facile vinyl dimerisation reaction.

These studies indicated that over the $Rh/CeO_2/SiO_2$ catalyst, surface vinyl derived from vinyl probes was an extremely effective initiator of methylene polymerisation. The "alkenyl mechanism" for the FT reaction was proposed, in which chain growth is initiated by a vinyl + methylene coupling, proceeds by alkenyl + methylene coupling, and terminates via hydrogenation of the alkenyl to yield the 1-alkene (15). This mechanism, shown in Fig. 1, has a number of advantages over the alkyl mechanism, since it can explain the formation of branched products (for example, by allyl isomerisation); the low amount of C_2 products (the mechanism for the formation of the C_2 initiator is different from the subsequent chain growth steps); and the release of 1-alkenes as primary products (by a favourable hydrogenation reaction). Some of this work has been reviewed recently (20).

The studies described below have been carried out to determine whether vinyl initiation of FT chain growth is unique to rhodium-catalysed syntheses, or whether it has wider generality. A ruthenium on silica catalyst was chosen for this study, since this is a more "typical" FT catalyst, with a high activity and selectivity for hydrocarbon formation; rhodium also catalyses oxygenate production.

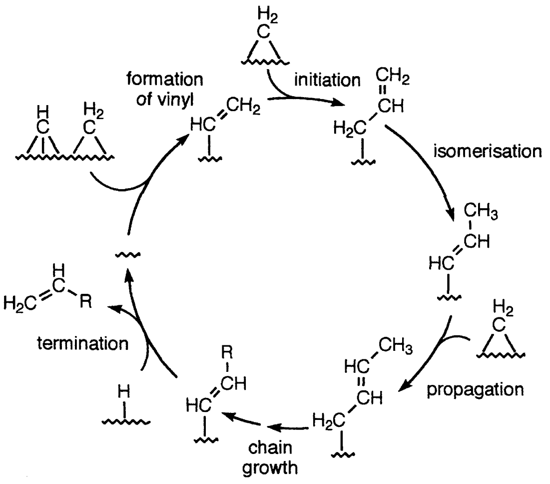

FIG. 1. The alkenyl mechanism for the stepwise polymerisation of methylene in the Fischer–Tropsch reaction.

METHODS

Catalyst Preparation and Pretreatment

A Ru (4%)/SiO_2 catalyst was prepared by incipient wetness impregnation of silica (Davisil grade 645) with a solution of ruthenium trichloride hydrate (PGP Industries (Ireland) Ltd) in methanol, using a weight loading of 4%. The impregnated sample was dried at 80°C in air. Prior to CO hydrogenation, the dried sample (1.0 g) was packed into a fixed-bed microreactor where it was reduced under a steady stream of hydrogen (1 atm, 1000 $cm^3\ h^{-1}$), by programmed heating (4°C min^{-1}) from room temperature to 400°C. It was held at 400°C for 4 h and then cooled to the reaction temperature (typically 180°C).

Catalyst Characterisation

Static physisorption and chemisorption measurements were performed using a Micromeritics ASAP 2000 instrument. Research grade purity gases were employed without further purification.

The BET area was obtained from N_2 adsorption at −196°C (77 K). The Ru (4%)/SiO_2 catalyst exhibited a BET surface area of 295 $m^2\ g^{-1}$ before reduction. H_2 chemisorption isotherms were measured at 35°C in the pressure range 75–225 mmHg. The chemisorption experiments were carried out after the catalyst had been reduced in H_2 (50–70 $cm^3\ min^{-1}$) at 400°C for 4 h (heating rate 4°C min^{-1}) and then evacuated at 400°C for 2 h and for 0.5 h at room temperature. The quantity of gas chemisorbed was found by extrapolation of the linear portion of the adsorption isotherm to zero pressure (5 points from 75 to 225 mmHg).

The ruthenium metal area was found to be 1.3 $m^2\ g^{-1}$ at 35°C, which corresponds to a metallic dispersion of 8.5%. Ruthenium catalysts prepared from ruthenium trichloride typically give low dispersions which may result from the retention of some surface chlorine on the metal surface after reduction at 400°C (21).

Reaction and Analysis

Reaction conditions. CO hydrogenation reactions were carried out at 180°C, 1 atm, $H_2/CO = 2$, total flow rate 500 $cm^3\ h^{-1}$. The total carbon conversion was approximately 10%. After 6–7 h reaction time under syn gas, the catalyst required reactivation by reduction under H_2 for 4 h (heating rate 4°C min^{-1}). A freshly prepared catalyst required two syn gas reaction/reactivation cycles followed by 1.5 h on-stream to attain steady-state activity.

Probe molecule introduction. Vinyl bromide (98%) and ethyl bromide (99+%) were obtained from Aldrich, and ethene (CP Grade) was obtained from BOC. Doubly labelled ethene ($^{13}C_2H_4$; 99% ^{13}C) and vinyl bromide ($^{13}C_2H_3Br$; 99% ^{13}C) were obtained from MSD of Canada. Six pulses of the probe (each 1.14×10^{-5} mol) were introduced into the syn gas upstream of the reactor via a gas syringe (or liquid microsyringe for ethyl bromide) at 5 min intervals. The effective ratio of probe to converted CO was approximately 1 : 6.

Product sampling. For each probe molecule study, product samples were collected before, during, and after probe addition. The reaction times corresponded to 1.5, 3.0, and 4.5 h, respectively. In the absence of added probe, a sample of the product gases (250 μl) was collected via a gas syringe for off-line GC analysis. In the presence of probe, a sample of the product gases was collected at a predetermined time after the final pulse of probe. GC–MS analysis required a higher concentration of products than could be obtained by direct sampling, therefore, the products were collected in a liquid nitrogen trap for a period of 0.5 h. During a probe experiment, collection was at low temperature for the entire duration of probe addition.

Analytical instrumentation. Quantitative analysis of the reaction products was carried out on a Perkin Elmer 8700 GC fitted with a Supelco SPB-1 column (60 m × 0.53 mm × 5 μm) and a flame ionisation detector. The detector was precalibrated with external standards of known concentration. ^{13}C incorporation was analysed using a Hewlett Packard 5890-5971 A GC–MS fitted with an electron-impact ion source, a hyperbolic quadrupole mass filter, and an electron multiplier detector. C_4 to C_7 hydrocarbons were separated on a Chrompack CP-Sil-5 CB column (50 m × 0.32 mm × 5 μm), and C_1 to C_3 hydrocarbons were separated using the CP-Sil-5 CB column coupled to a Chrompack PLOT alumina column (30 m × 0.32 mm).

RESULTS

CO Hydrogenation

Carbon monoxide was hydrogenated to hydrocarbons over Ru/SiO_2 at 180°C. 1-Alkenes and alkanes were the major products; trace amounts of oxygenates (methanol, ethanal, and ethanol) were also detected. Small amounts of 2-alkenes were also formed, though the amounts produced were much lower than predicted for thermodynamic equilibrium. The only branched hydrocarbon produced in significant amounts was 2-methyl-2-butene. A plot of log (W/n) against n (W, weight fraction; n, number of carbon atoms in that fraction) for the hydrocarbon products, showed typical Anderson–Schulz–Flory (ASF) behaviour for a ruthenium-catalysed FT reaction (Fig. 2) with a very low C_2 fraction, a slightly low C_3 fraction, and a monotonic decrease from $n = 4$ to 8, indicative of a step-wise polymerisation. A typical value for the chain growth probability (α), based on the C_4–C_8 fractions, was found to be 0.65 from the gradient and 0.63 from the intercept.

The catalyst reached steady-state activity after the initial activation period. As observed by other workers in the field, there was a slow drop in activity with time, illustrated in the bar graphs before and after addition of an ethene probe in Fig. 3a. After 6–7 h on stream the catalyst was reactivated by heating under hydrogen.

Addition of Unlabelled Probe Molecules

Addition of vinylic probes to the CO hydrogenation reaction led to a significant change in the product distribution, as shown in Fig. 3. Each graph shows three data sets: the first represents the product distribution at steady state; the second shows the distribution during addition of the vinylic probe; and the third shows the return of the system to

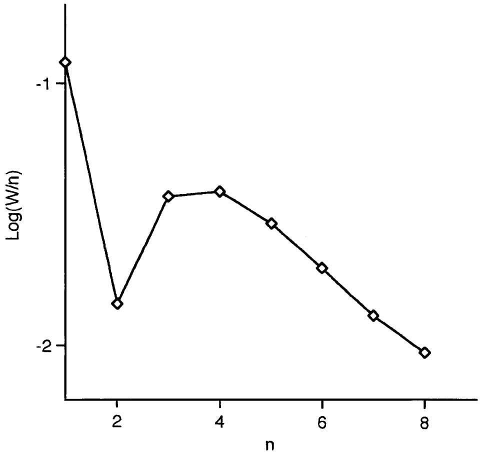

FIG. 2. Anderson–Schulz–Flory plot of the formation of hydrocarbons from CO hydrogenation, where W is the weight fraction of products having n carbon atoms.

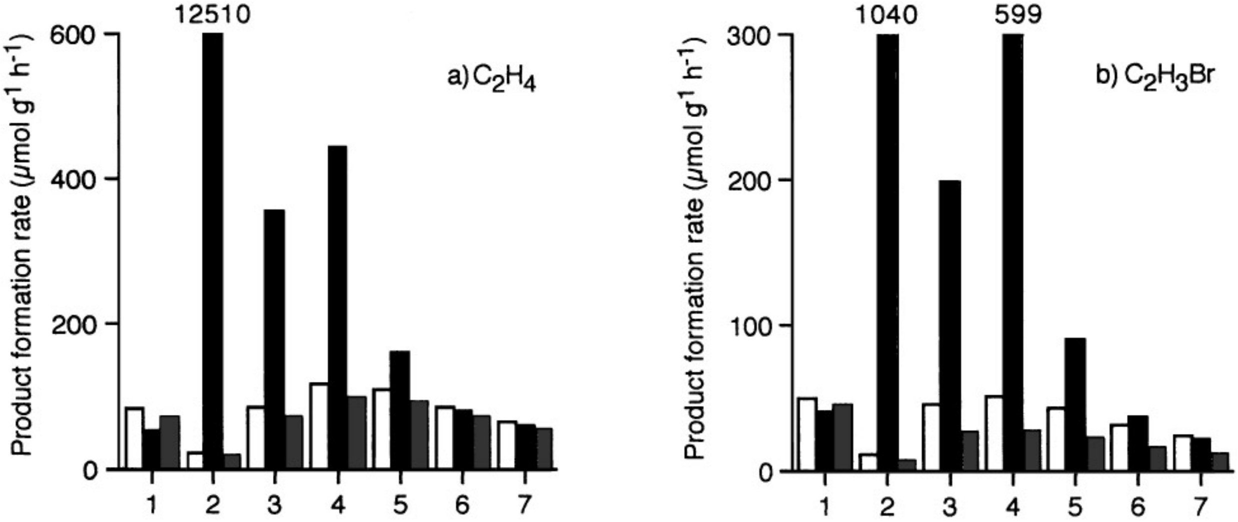

FIG. 3. Bar graphs showing product formation rate (y-axis: μmol(carbon) g^{-1} h^{-1}) against the number of carbon atoms in the product hydrocarbons (x-axis): in each case the left-hand bar represents the rate before vinyl probe addition, the middle bar is during probe addition, and the right-hand bar is after addition, when the system has again returned to equilibrium.

steady state after the probe had been transmitted through the catalyst. The addition of either ethene or vinyl bromide caused an increase in the formation rate of the C_2 to C_5 hydrocarbons (with the C_2 and C_4 formation rates being most enhanced) and a slight decrease in the methane formation rate. Addition of vinyl bromide also increased the rate of formation of the C_6 fraction. After ethene addition, the product distribution returned close to its preprobe addition value; however, after vinyl bromide addition the product formation rates were approximately halved. The chain growth probability decreased from 0.65 to 0.42 during vinyl bromide addition and to 0.51 during ethene addition. This drop was transient and the chain growth probability returned to its initial value approximately 3 min after the pulse of probe.

Addition of ethyl bromide to the CO hydrogenation reaction resulted only in an increase in the formation rate of the C_2 fraction, as shown in Fig. 4. After ethyl bromide addition, the product formation rates fell to approximately half of the preprobe addition values. The chain growth probability decreased slightly from 0.68 to 0.62 during addition of ethyl bromide.

Meaningful quantification of unreacted probe was not possible due to the probe being added in "pulses," so it was not possible to measure the amount of probe consumed; however, some unreacted probe was detected in every experiment.

Addition of $^{13}C_2$-Labelled Probe Molecules

The incorporation of $^{13}C_x$ ($x = 0, 1, 2, \ldots n$) from $^{13}C_2H_4$ or $^{13}C_2H_3Br$ into the C_n hydrocarbons formed over Ru/SiO$_2$ at 180°C is shown in Tables 1 and 2. As it was not possible to analyse all the products simultaneously, two identical experiments were required for full characterisation; the $C_{\geq 3}$ hydrocarbon fractions were analysed from the first experiment and the C_1 and C_2 fractions were analysed from the second. The results are given as the percentage of $^{13}C_x$ of the total C_n fraction. The expected natural abundance $^{13}C_x$ incorporation is zero for all but $x = 1$; the natural abundance $^{13}C_1$ levels are therefore given for each product in parentheses. They are calculated on the basis that for a C_n hydrocarbon $(1.1 \times n)\%$ of the amount of $^{13}C_0$ is $^{13}C_1$. Thus

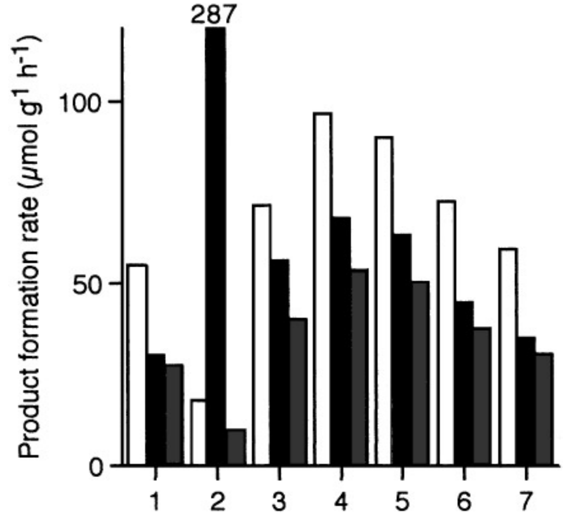

FIG. 4. Bar graphs showing product formation rate (y-axis: μmol(carbon) g^{-1} h^{-1}) against the number of carbon atoms in the product hydrocarbons (x-axis): in each case the left-hand bar represents the rate before ethyl bromide probe addition, the middle bar is during probe addition, and the right-hand bar is after addition.

TABLE 1

Incorporation of $^{13}C_x$ from $^{13}C_2H_4$ Probe[a]

x	0	1[b]	2	3	4	5	6	7	8
Methane[c]	90	10(1)							
Ethene[c]	4	9(0)	87						
Ethane[c]	6	0(0)	94						
Propene	17	10(1)	57	17					
1-Butene	35	5(2)	34	9	18				
Butane	42	5(2)	31	9	14				
cis-2-Butene	6	0(0)	5	2	86				
1-Pentene	49	5(3)	31	5	7	4			
Pentane	50	8(3)	26	6	6	5			
trans-2-Pentene	37	2(2)	35	7	11	8			
cis-2-Pentene	19	3(1)	12	7	26	33			
2-*Me*-2-Butene	17	5(1)	12	6	38	22			
1-Hexene	57	6(4)	25	4	4	2	2		
Hexane	59	6(4)	23	4	4	1	2		
trans-2-Hexene	49	9(3)	23	1	7	6	6		
cis-2-Hexene	33	3(2)	16	3	12	8	26		
1-Heptene	70	7(5)	17	3	2	1	1	0	
Heptane	72	7(6)	15	3	2	1	1	0	
trans-2-Heptene	74	5(6)	19	1	0	0	1	0	
cis-2-Heptene	60	7(5)	15	2	5	1	4	8	
1-Octene	81	8(7)	8	1	0	0	0	0	0

[a] $^{13}C_x$ incorporation was not calculated for some products either because insufficient levels were detected or because the GC resolution was poor.

[b] Figures in parentheses are the expected percentage $^{13}C_1$ levels at natural abundance.

[c] Data found from a separate experiment operating under identical conditions.

in Table 1 for a methane content of 90% $^{13}C_0$ one would expect ca. $(0.9 \times 61)\%$ or 1% (rounded up) $^{13}C_1$; similarly, for a C_5 hydrocarbon such as 1-pentene which has a content of 50% $^{13}C_0$ one would expect $(0.5 \times 5.5)\% = 2.75$ or 3% (rounded up) $^{13}C_1$.

It can be seen from Tables 1 and 2 that the patterns of $^{13}C_x$ incorporation are similar, whether derived from $^{13}C_2H_4$ or $^{13}C_2H_3Br$. $^{13}C_2$ incorporation is the most significant and is far higher than either $^{13}C_1$ or $^{13}C_3$ incorporation. In contrast to the results obtained over rhodium catalysts (15), $^{13}C_1$ incorporation is higher than expected from natural abundance, and the amounts of $^{13}C_x$ $(x > 2)$ are also highly significant. The labelling patterns within a particular C_n fraction are not identical; high $^{13}C_4$ incorporation is found in *cis*-2-butene and also in the $C_{\geq 5}$ *cis*-2-alkenes.

DISCUSSION

CO Hydrogenation

The products formed by the catalytic hydrogenation of CO over Ru/SiO_2 were typical for a ruthenium-catalysed FT synthesis. The activity was approximately double that of the $Rh/CeO_2/SiO_2$ catalysts used in previous studies (15); the probability of chain growth was higher ($Rh/CeO_2/SiO_2$, $\alpha = 0.52$; Ru/SiO_2, $\alpha = 0.65$); and the proportion of 1-alkenes was higher. The latter observation indicates that the Ru/SiO_2 catalyst was less strongly hydrogenating than the $Rh/CeO_2/SiO_2$ catalyst. *cis*- and *trans*-2-alkenes were formed in very low amounts, also suggesting that secondary isomerisation reactions are not well catalysed over Ru/SiO_2 under these conditions.

Addition of Unlabelled Probe Molecules

The effect of adding a vinylic probe was to increase the amount of $C_{\geq 2}$ hydrocarbons produced, as shown in Fig. 3. This strongly suggests that the species derived from the probes become involved in the chain growth process. The relative increase of each fraction becomes less as the molecular weight of the fraction increases, hence very little enhancement was observed for the fractions $C_{>6}$. The greatest rate increases were obtained for the C_2 and C_4 fractions. The formation of much ethane indicates that probe hydrogenation/hydrogenolysis occurs; the enhanced formation of C_4 hydrocarbons indicates that dimerisation is significant.

TABLE 2

Incorporation of $^{13}C_x$ from $^{13}C_2H_3Br$ Probe[a]

x	0	1[b]	2	3	4	5	6	7	8
Methane[c]	94	6(1)							
Ethene[c]	17	4(0)	79						
Ethane[c]	2	0(0)	98						
Propene	32	0(1)	45	23					
Propane	34	8(1)	35	23					
1-Butene	41	7(2)	22	13	17				
Butane	44	7(2)	22	13	14				
trans-2-Butene	20	4(1)	21	15	40				
cis-2-Butene	5	2(0)	5	7	81				
1-Pentene	56	7(3)	17	8	8	4			
Pentane	53	7(3)	18	8	8	6			
trans-2-Pentene	35	7(2)	21	11	16	11			
cis-2-Pentene	30	5(2)	15	8	22	18			
2-*Me*-2-Butene	13	2(1)	7	4	39	35			
1-Hexene	67	8(4)	12	5	4	2	2		
Hexane	61	8(4)	12	7	6	3	3		
trans-2-Hexene	50	8(3)	16	8	8	6	5		
cis-2-Hexene	48	7(3)	14	7	9	7	9		
1-Heptene	80	8(6)	6	2	2	1	1	0	
3-Heptene	51	9(4)	13	7	7	5	4	4	
Heptane	75	8(6)	8	3	3	2	1	0	
trans-2-Heptene	71	8(5)	9	4	3	2	2	1	
cis-2-Heptene	71	8(5)	9	3	3	2	2	1	
1-Octene	90	8(8)	1	0	0	0	0	0	0
cis-2-Octene	89	7(8)	1	1	0	0	0	1	0

[a] $^{13}C_x$ incorporation was not calculated for some products either because insufficient levels were detected or because the GC resolution was poor.

[b] Figures in parentheses are the expected percentage $^{13}C_1$ levels at natural abundance.

[c] Data found from a separate experiment operating under identical conditions.

The rate of methanation showed a small decrease upon addition of a vinylic probe. Methane is probably formed by hydrogenation of surface methylene; a consequence of the low metallic surface area of the Ru/SiO_2 catalyst is that there will be a strong competition for active sites among the various processes that occur, including the hydrogenation of surface methylene.

The only effect of ethyl bromide was to increase the ethane formation rate (Fig. 4). This indicates that, although probe hydrogenolysis occurs, and the C–Br bond is cleaved on the surface, presumably with the formation of surface ethyls, there is no incorporation into the Fischer–Tropsch products. There is therefore a sharp contrast between the effects of saturated and unsaturated probes, and the rate enhancement observed during vinyl bromide addition cannot be attributed to an *alkyl* intermediate derived from the vinyl.

These observations are similar to those we made for rhodium-based systems (15) and are again more consistent with the alkenyl mechanism for Fischer–Tropsch chain growth (Fig. 1), in which surface vinyls initiate and alkenyl groups are the chain carriers, than the alkyl mechanism, in which surface alkyl groups initiate and propagate chain growth.

Addition of organic bromides led to a substantial deactivation of the ruthenium catalyst. We suggest that this is associated with bromide blocking active sites on the metal. Although the data are not yet complete, EXAFS and SuperESCA studies indicate the presence of bromide on a rhodium catalyst after exposure to organic bromides. It is to be expected that similar effects will occur over ruthenium.

Addition of $^{13}C_2$-Labelled Vinylic Probe Molecules

$^{13}C_2$ incorporation. The major effect of the addition of a $^{13}C_2$-labelled vinylic probe was the large amount of $^{13}C_2$ present in virtually all the hydrocarbon products (data in Tables 1 and 2). This was always much greater than the amounts of $^{13}C_1$ and $^{13}C_3$ found, and one may safely assume that it arises from the incorporation of $1 \times {}^{13}C_2$ unit, rather than from $2 \times {}^{13}C_1$ units. Similar levels of $^{13}C_2$ incorporation were found from both $^{13}C_2H_4$ and $^{13}C_2H_3Br$, consistent with the two labelled carbons being incorporated as a unit, with an unbroken ^{13}C–^{13}C bond. The proportion of $^{13}C_2$-labelled products decreased as the hydrocarbon chain length increased; this is consistent with initiation by the $^{13}C_2$-unit, but is inconsistent with such C_2 units being involved in the propagation reactions. The increase in product formation rate also suggests that the vinylic probes are behaving as initiators, in the same way as we found for the reactions over $Rh/CeO_2/SiO_2$ catalysts (15).

$^{13}C_1$ incorporation. The data in Tables 1 and 2 also show that the amount of $^{13}C_1$ present in the hydrocarbon products is significantly greater than natural abundance; thus the $^{13}C_2$-labelled probes undergo some C–C cleavage to $^{13}CH_x$ units over the ruthenium catalyst. The detection of 5–10% $^{13}CH_4$ in the products supports this conclusion. The observed changes in the rate of formation of methane therefore reflect the balance between probe cleavage and a suppression of methanation on the surface. The ability of ruthenium to cleave C–C bonds has previously been noted by other authors (22, 23). Both these two reactions have been reported over Ru/SiO_2 catalysts during ethene addition to a FT reaction (24).

$^{13}C_4$ incorporation. As we observed in our experiments over rhodium, $^{13}C_4$ incorporation is also significant, especially in *cis*-2-butene where it accounts for ca. 80% of the total product. These levels are too high to arise from the incorporation of $4 \times {}^{13}C_1$ units and must indicate a dimerisation of two $^{13}C_2$ units derived from the probes. The high levels of ^{13}C label in the thermodynamically least favourable 2-alkene, and the relative inability of the ruthenium catalyst to catalyse secondary isomerisation reactions suggest that *cis*-2-butene is the kinetically favoured product of dimerisation.

Only very small amounts of *cis*-2-butene are formed in the reaction and thus one must guard against overinterpretation. However, the evidence favours a formation route by coupling of two surface vinyls to 1,3-butadiene, which is then selectively hydrogenated to give *cis*-2-butene. Vinyl–vinyl coupling to form 1,3-butadiene has been observed over clean metal surfaces under ultra high vacuum conditions (25) and in well-characterised mononuclear organometallic complexes (26). $^{13}C_4$ incorporation into hydrocarbon products was also found to occur during vinylic probe addition to Fischer–Tropsch reactions over rhodium catalysts; there, as here over ruthenium, 1,3-butadiene was not detected as a product (15). When 1,3-butadiene was added as a probe to a carbon monoxide hydrogenation over Ru/SiO_2 in a separate experiment, it was found that the formation rate of *cis*-2-butene was increased by 140, while that of *trans*-2-butene was increased by a factor of almost 1500; no unreacted 1,3-butadiene was observed.

Since the reductive elimination of two groups on two adjacent metal atoms is symmetry forbidden, we suggest that two vinyls couple at a single metal centre to form *s*-*cis*-1,3-butadiene bound to the metal surface; a 1 : 4 hydrogenation can then occur to yield *cis*-2-butene. The preferential formation of *trans*-2-butene, when butadiene itself is added directly, suggests that prior to hydrogenation 1,3-butadiene coordinates in a different manner (perhaps to two metal centres in the *s*-*trans*- conformation), which does not interconvert (27, 28). Similar vinyl plus alkenyl couplings could account for $^{13}C_4$ incorporation into the $C_{\geq 5}$ hydrocarbons.

$^{13}C_3$, $^{13}C_5$, and $^{13}C_6$ incorporation. Analysis of the products shows the presence of small amounts of $^{13}C_3$-, $^{13}C_5$-, and even some $^{13}C_6$-labelled hydrocarbons. The

$^{13}C_6$-labelled materials (such as the hexenes, present in trace amounts) presumably arise from some vinyl probe trimerisation, which may be related to the dimerisation that gives rise to $^{13}C_4$-labelled products. One possibility for the formation of $^{13}C_3$-labelled products is that C–C cleavage can occur of the $^{13}C_4$-labelled materials. The $^{13}C_5$-labelled hydrocarbons can arise by similar vinyl plus alkenyl couplings to the vinyl plus vinyl discussed above. Another possibility is that cleavage of the vinylic probes occurs with formation of methylene species which can then take part in chain growth.

We suggest that the formation of these products involves "secondary" reactions. Secondary processes, in particular the reabsorption of olefins, are common in many Fischer–Tropsch systems and have recently been extensively investigated by groups at Exxon and at Shell (29). Since our aim has been to obtain mechanistic information rather than to maximise activity, our work has been carried out under conditions where the products are largely 1-alkenes and "primary" reactions are maximised.

The alkenyl mechanism for the Fischer–Tropsch reaction over Ru/SiO$_2$. The aim of this work was to determine whether the alkenyl mechanism was operative for hydrocarbon formation from CO/H$_2$ over ruthenium as well as over rhodium catalysts.

In brief, the alkenyl mechanism (Fig. 1, and Refs. 15, 20) proposes that a C$_2$ surface vinyl (–CH=CH$_2$) species is formed by combination of surface methyne (CH) and methylene (>CH$_2$) which arise from the hydrogenation of adsorbed CO. In the first step of the polymerisation cycle, the vinyl then reacts with surface methylene to give a surface allyl, which isomerises to σ-propenyl. The σ-propenyl then reacts further with methylene to form a new allylic species which then again isomerises to an alkenyl; chain termination can occur in several ways, since α-olefins are the chief products under our mild conditions, the most likely is by reaction of the alkenyl with a surface hydride. An unexpected feature of the cycle is the σ-allyl to σ-propenyl isomerisation; however, such reactions are well known for organometallic compounds (30).

The results described here show that surface vinyl, derived from either vinyl bromide or ethene, significantly enhances the productivity of an FT synthesis over Ru/SiO$_2$. In addition, labelling studies show conclusively that the probe can be incorporated into the product hydrocarbons as a C$_2$ unit.

To examine the role of the probe in FT chain growth further, a quantitative approach was used, based upon a steady-state treatment of the alkenyl mechanism, the details of which have been described previously (15). The mass balance Eq. [1] is obtained from a consideration of the propagation and termination steps (rate constants k_p and k_t, respectively) shown in Fig. 5. $[A_n]$ is the concentration of surface alkenyls having n carbon atoms, $[M]$ is the concentration of surface methylene, and $[H]$ is the concentration of surface hydride. The chain growth probability is given by α.

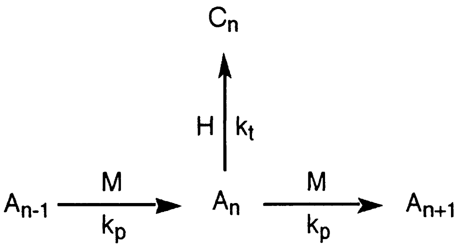

FIG. 5. Representation of the key propagation (k_p) and termination (k_t) steps of the alkenyl mechanism for the Fischer–Tropsch polymerisation, used in the steady-state kinetic treatment (text, Eq. [1]), where A_n is the concentration of alkenyl C$_n$ species, M is the concentration of methylene (CH$_2$), and H is the concentration of active hydrogen in the surface.

$$\frac{[A_n]}{[A_{n-1}]} = \frac{k_p[M]}{k_p[M] + k_t[H]} = \alpha. \qquad [1]$$

Since we also observe vinyl–vinyl (and vinyl–alkenyl) coupling during probe addition a third denominator term, given by $k_c[A_2]$, can be included to model the situation at the instant of probe addition when $[A_2]$ is very high. The inclusion of this term accounts for the transient decrease in the chain growth probability when a vinylic probe is added to a Fischer–Tropsch reaction.

Using Eq. [1], it is then possible to calculate the expected level of $^{13}C_2$ incorporation in the different fractions $\{^{13}C_2–C_n\}$, based upon how much of the surface vinyl is $^{13}C_2$-labelled; this percentage is described as $\left\{^{13}C_2\text{-}A_2\right\}$. For example, if α is 0.7 and initially 70% of the surface vinyl is assumed to be $^{13}C_2$-labelled:

$$\begin{aligned}
\left\{^{13}C_2–C_2\right\} &= \left\{^{13}C_2\text{-}A_2\right\} = 70\%;\\
\left\{^{13}C_2–C_3\right\} &= \left\{^{13}C_2\text{-}A_3\right\} = \alpha\left\{^{13}C_2\text{-}A_2\right\}\\
&= 0.7 \times 70 = 49\%;\\
\left\{^{13}C_2–C_4\right\} &= \left\{^{13}C_2\text{-}A_4\right\} = \alpha\left\{^{13}C_2\text{-}A_3\right\}\\
&= 0.7 \times 49 = 34\%, \text{etc.}
\end{aligned}$$

It can be seen that this relationship predicts that the fraction of $^{13}C_2$-labelled products $\{^{13}C_2–C_n\}$ will decrease as the chain length (n) of the products increases, as observed experimentally. The theoretical and experimental $^{13}C_2$ incorporation data derived from each probe are compared graphically in Fig. 6. As for the experiments using various $^{13}C_2$ vinyl probes over rhodium (15), there is good agreement between the experimental and the theoretical curves for vinyl bromide, except for a dip at C$_4$, which arises because vinyl–vinyl coupling has not been accounted for. For ethene as probe the experimental values show higher than expected $^{13}C_2$ incorporation in the C$_5$–C$_7$

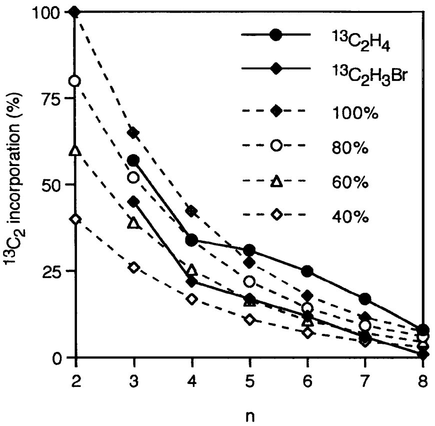

FIG. 6. Comparison between experimental (bold lines) and theoretical (dotted lines) values for $^{13}C_2$ incorporation into hydrocarbons with *n* carbons from vinyl bromide and ethene as probes.

hydrocarbons. This discrepancy must arise from some $^{13}C_2$-containing products being formed by a second mechanism in the ruthenium-catalysed reaction. The nature of that process, currently under investigation, is not yet clear, but it is unlikely to be due to the incorporation of $2 \times {}^{13}C_1$ units, since the amount of probe cleavage is small, $<10\%$.

CONCLUSION

Experiments with vinyl and ethyl probes have shown that carbon monoxide hydrogenation over ruthenium on silica incorporates vinylic species, but not ethyl. This is consistent with a predominant role for an alkenyl mechanism for the Fischer–Tropsch reaction, involving a vinyl initiation and methylene plus alkenyl propagation, similar to the one we proposed for the analogous rhodium catalysed reactions. The data are also consistent with those of other workers who previously suggested (undefined) C_2 intermediates to play important roles in Fischer–Tropsch reactions (31). The main differences between rhodium and ruthenium are that ruthenium is more active for homologation, gives fewer isomerisation and hydrogenation side reactions, and has a higher selectivity towards hydrocarbons and especially l-alkenes. However, the ruthenium-catalysed reactions do show some C–C cleavage of the vinylic probe, a phenomenon which is almost entirely absent over rhodium.

ACKNOWLEDGMENTS

We thank the Royal Society, the SERC (EPSRC), and the EU Human Capital and Mobility scheme (Contract ERBCHRXCT930147) for support of this work.

REFERENCES

1. Kaminsky, M. P., Winograd, N., Geoffroy, G. L., and Vannice, M. A., *J. Am. Chem. Soc.* **108**, 1315 (1986).
2. Fischer, F., and Tropsch, H., *Brennstoff Chem.* **7**, 97 (1926).
3. Biloen, P., Helle, J. N., and Sachtler, W. M. H., *J. Catal.* **58**, 95 (1979).
4. Brady, R. C., III, and Pettit, R., *J. Am. Chem. Soc.* **102**, 6181 (1980).
5. Brady, R. C., III, and Pettit, R., *J. Am. Chem. Soc.* **103**, 1287 (1981).
6. McCandlish, L. E., *J. Catal.* **83**, 362 (1983).
7. Joyner, R. W., *Catal. Lett.* **1**, 307 (1988).
8. Maitlis, P. M., *J. Organomet. Chem.* **500**, 239 (1995).
9. Saez, I. M., Andrews, D. G., and Maitlis, P. M., *Polyhedron* **7**, 827 (1988).
10. Saez, I. M., Meanwell, N. J., Nutton, A., Isobe, K., Vázquez de Miguel, A., Bruce, D. W., Okeya, S., Andrews, D. G., Ashton, P. R., Johnstone, I. R., and Maitlis, P. M., *J. Chem. Soc., Dalton Trans.* 1565 (1986).
11. Martinez, J., Adams, H., Bailey, N. A., and Maitlis, P. M., *J. Chem. Soc., Chem. Commun.* 286 (1989).
12. Martinez, J., Gill, J. B., Adams, H., Bailey, N. A., Saez, I. M., Sunley, G. J., and Maitlis, P. M., *J. Organomet. Chem.* **394**, 583 (1990).
13. Calhorda, M. J., Brown, J. M., and Cooley, N. A., *Organometallics* **10**, 1431 (1991); see also Collman, J., Hegedus, L. S., Norton, J. R., and Finke, R. G., *in* "Principles and Applications of Organo-Transition Metal Chemistry," p. 322 *et seq*. University Science Books, Mill Valley, CA, 1987; Evitt, E. R., and Bergman, R. G., *J. Am. Chem. Soc.* **102**, 7003 (1980).
14. Turner, M. L., Byers, P. K., Long, H. C., and Maitlis, P. M., *J. Am. Chem. Soc.* **115**, 4417 (1993).
15. Turner, M. L., Long, H. C., Shenton, A., Byers, P. K., and Maitlis, P. M., *Chem. Eur. J.* **1**, 549 (1995).
16. Zaera, F., and Bernstein, N., *J. Am. Chem. Soc.* **116**, 4881 (1994).
17. Zhou, X.-L., and White, J. M., *J. Phys. Chem.* **96**, 7703 (1992).
18. Zhou, X.-L., Schwaner, A. L., and White, J. M., *J. Am. Chem. Soc.* **115**, 4309 (1993).
19. Liu, Z.-M., Zhou, X.-L., Buchanan, D. A., Kiss, J., and White, J. M., *J. Am. Chem. Soc.* **114**, 2031 (1992).
20. Maitlis, P. M., Long, H. C., Quyoum, R., Turner, M. L., and Wang, Z.-Q., *J. Chem. Soc., Chem. Commun.* 1 (1996).
21. Lu, K., and Tatarchuk, B. J., *J. Catal.* **106**, 176 (1987).
22. Rodriguez, E., Leconte, M., Basset, J.-M., Tanaka, K., and Tanaka, K.-I., *J. Am. Chem. Soc.* **110**, 275 (1988).
23. Rodriguez, E., Leconte, M., and Basset, J.-M., *J. Catal.* **132**, 472 (1991).
24. Morris, S. R., Moyes, R. B., Wells, P. B., and Whyman, R., *J. Catal.* **96**, 23 (1985).
25. Yang, M. X., Eng, J., Kash, P. W., Flynn, G. W., Bent, B. E., Holbrook, M. T., Bare, S. R., Gland, J. L., and Fischer, D. A., *J. Phys. Chem.* **100**, 12431 (1996).
26. Wang, Z.-Q., Turner, M. L., Kunicki, A. R., and Maitlis, P. M., *J. Organomet. Chem.* **488**, C11 (1995), and unpublished data.
27. Wells, P. B., and Bates, A. J., *J. Chem. Soc.(A)* 3064 (1968).
28. Bond, G. C., Webb, G., Wells, P. B., and Winterbottom, J. M., *J. Chem. Soc.* 3218 (1965).
29. Iglesia, E., Reyes, S. C., Madon, R. J., and Soled, S. L., *Adv. Catal.* **39**, 221 (1993); Kuipers, E. W., Scheper, C., Wilson, J. H., Vinkenburg, I. H., and Oosterbeek, H., *J. Catal.* **158**, 288 (1996).
30. Deeming, A. J., Shaw, B. L., and Stainbank, R. E., *J. Chem. Soc. (A)* 374 (1971); Wang, L. S., and Cowie, M., *Can. J. Chem.* **73**, 1058 (1995).
31. See, for example, Kummer, J. T., Spencer, W. B., Podgurski, H. H., and Emmett, P. H., *J. Am. Chem. Soc.* **73**, 564 (1951); Kummer, J. T., and Emmett, P. H., *J. Am. Chem. Soc.* **75**, 5177 (1953); Kobori, Y., Yamasaki, H., Naito, S., Onishi, T., and Tamaru, K., *J. Chem. Soc., Faraday Trans. I* **78**, 1473 (1982); Snel, R., and Espinoza, R. L., *J. Mol. Catal.* **43**, 237 (1987); Mims, C. A., McCandlish, L. E., and Melchior, M. T., *Catal. Lett.* **1**, 121 (1988); Cavalcanti, F. A. P., Oukaci, R., Wender, I., and Blackmond, D. G., *J. Catal.* **123**, 270 (1990); Mims, C. A., Krajewski, J. J., Rose, K. D., and Melchior, M. T., *Catal. Lett.* **7**, 119 (1990); Krishna, K. R., and Bell, A. T., *Catal. Lett.* **14**, 305 (1992).